1 A Method to Decipher the Time Distribution in Astronomically Forced Sedimentary **Couplets** 2 Chao Ma^{1,6*}, Stephen R. Meyers¹, Linda A. Hinnov², James S. Eldrett³, Steven C. 3 Bergman^{4,5}, Daniel Minisini⁴ 4 5 ¹Department of Geoscience, University of Wisconsin–Madison, 1215 West Dayton Street, 6 7 Madison, Wisconsin 53706, USA. ²Department of Atmospheric, Oceanic, and Earth Sciences, George Mason University, Fairfax, 8 VA, 22030, USA. 9 ³Shell International Exploration & Production B.V, 1Lange Kleiweg 40, 2288 GK Rijswijk, 10 Netherlands 11 ⁴Shell International Exploration and Production, 3333 Highway 6 South, Houston, TX, 77082, 12 USA 13 ⁵SCB GeoSciences, 20625 Chautauqua Beach Rd, SW, Vashon, WA 98070, USA 14 15 ⁶Now at Department of Computer Science, University of Idaho, Moscow, ID, 83843, USA *e-mail: chao@uidaho.edu 16

Abstract

Sedimentary couplets that are generated by astronomical forcing are common in pelagic and hemipelagic depositional settings. This study disentangles the time scales (sedimentation rates) of the two lithofacies that contribute to such astronomically-forced couplets, by introducing the Alpha method. This new method can be applied to precession or obliquity-forced sedimentary records, and compares the frequency modulation of an astronomical cycle model with the thicknesses of the couplets. The method is demonstrated on a synthetic model of a precession index-forced succession of limestone-marlstone couplets. Finally, the methods is applied to two case studies: for the Middle Cenomanian Eagle Ford Formation (Iona-1 core, Texas), sedimentation rates are estimated as 0.85-1.02 cm/kyr for the marlstone and 4.70-5.65 cm/kyr for the limestone; for the Middle Eocene IODP Expedition 342 Site U1408, sedimentation rates are 1.70-1.84 cm/kyr for the white nannofossil ooze and 2.54-2.75 cm/kyr for the greenish nannofossil-rich clay. More generally, studies of paleoclimate and geochemical evolution at the sub-Milankovitch scale can benefit from this method.

Keywords

Alpha method, Milankovitch cycles, Eagle Ford Formation, Cretaceous, IODP U1408, Eocene

1. Introduction

Climatically driven rhythmic sedimentary bedding is found in strata throughout the Phanerozoic strata. An important source of such rhythms are the Milankovitch cycles, associated with astronomical variations in the orbits of the planets in the Solar System (recent reviews in Hinnov, 2013, 2018). The three major astronomical parameters affecting the Milankovitch cycles are the

Earth's precession index, obliquity and orbital eccentricity (Laskar et al., 2004), involving multiple components with periodicities ranging from ~20 kiloyears (kyr) to ~2,400 kyr (Laskar et al., 2004).

These parameters control the seasonal and latitudinal distribution of incoming solar radiation (insolation) received by the Earth, which affects the climate and subsequently the sedimentary environment.

A common sedimentary cycle is a couplet composed of two lithofacies, typically limestone and marlstone or shale, which are often generated by precession index forcing (Fischer 1986; Hilgen et al., 2014). Couplets interpreted as precession cycles have been documented in the Miocene of the Mediterranean (Krijgsman et al., 1995; Hilgen et al., 1995; Hilgen et al., 2014), Miocene continental (lacustrine) sections in Spain (Abels et al. 2009a,b), Miocene sediments of Ocean Drilling Program (ODP) Site 154 at Ceara Rise, the Cretaceous-Paleocene Zumaia section of the Basque basin in Spain (e.g., Dinarès-Turell et al., 2003; Kuiper et al., 2008; Batenburg et al., 2016), and in many of other pelagic and hemipelagic systems (e.g., Fischer 1986; Westphal and Munnecke, 2003; Westphal et al., 2008). The Research On Cretaceous Cycles Group (ROCC) (1986) identified four processes responsible for the development of rhythmic sedimentary couplets: (1) carbonate productivity, (2) terrigenous dilution, (3) redox conditions, and (4) bottom currents.

Ma et al. (2014) studied astronomically-driven sedimentation associated with Oceanic Anoxic Event 2 (OAE2) in the Western Interior Basin and observed precession and obliquity-forced lithologic couplets composed of carbonate-rich ("limestone") and carbonate-poor ("marlstone") hemicycles. Similar precession-forced couplets are found in the Cenomanian-Turonian strata of

Italy (Batenburg et al., 2016) and USA (e.g., Donovan et al., 2012; Eldrett et al., 2015a,b; Lehrmann et al., 2019). Variations in sediment and geochemistry within the couplet lithofacies are indications of signals at sub-astronomical time scales. Such signals offer the opportunity for studying potential diagenetic origin of the cyclicity and paleoclimate change from millennial to decadal scale (Davies et al., 2009; Westphal et al. 2010). An understanding of the time represented by the two lithofacies of the couplets is needed to reveal such an evolution and its rate(s).

69

70

71

72

73

74

75

76

77

78

79

80

81

82

83

84

85

63

64

65

66

67

68

In the present study, we describe a new approach to evaluate facies-specific sedimentation rates in astronomically-forced lithologic couplets, building on prior work. Previously, a linear inverse method known as the Gamma method (Kominz and Bond 1990, 1992; Kominz 1996) was developed to evaluate facies-dependent sedimentation rates in sequences of stratigraphic cycles. For example, consider the case where each cycle contains the same facies, and the sedimentation rate of a facies is assumed to be the same for all of the cycles. If the period of the stratigraphic cycles is constant, and the thickness of every facies in all cycles are known, then the sedimentation rates for each facies can be estimated (Kominz and Bond, 1990, 1992; Kominz, 1996). However, the Milankovitch cycles are quasi-periodic, with high frequency cycles (e.g., the precession index) modulated in frequency and amplitude by low frequency cycles (orbital eccentricity). This means that the constant period of the stratigraphic cycles assumed in the Gamma method does not strictly hold. Hinnov and Park (1998) explored the frequency modulation (FM) of Jurassic limestone-shale couplets. They found that the thickness of limestone or shale, or the couplets in their entirety, were influenced by the FM of the precession index by orbital eccentricity. But the FM method has not been applied to accurately resolve the distribution of time (sedimentation rates) between the two lithofacies in couplets.

Inspired by the above studies, we have designed an approach that we call the "Alpha method", which is a linear inverse approach that accounts for the FM of astronomical cycles to reconstruct the time represented by the two lithofacies in precession or obliquity driven couplets. We illustrate the method with a synthetic data and model (Section 2), and then apply it to two case studies: (1) the precession-dominated Middle Cenomanian Eagle Ford Formation (Section 3), and (2) the obliquity-dominated Middle Eocene of Expedition 342, Site U1408 (Section 4).

2. The Alpha Method

2.1 Assumptions and prior knowledge

The Alpha method is built on three fundamental assumptions: (1) There are no substantial discontinuities or hiatuses in the study interval; (2) facies-specific sedimentation rates are approximately constant across all couplets investigated, and (3) the general properties of the theoretical astronomical solution (e.g., Laskar et al., 2004) are valid for application in the study interval, even if a detailed understanding of the theoretical phase and amplitude are not known.

The following prior knowledge items must be known: (1) The sedimentary couplets are influenced by precession or obliquity forcing. (2) A range of plausible sedimentation rates for the facies has been determined. (3) The time constraints for each couplet (duration, related to precession or obliquity forcing) is known. (4) Age constraints of the studied interval are available to anchor the floating astronomical time scale, based on prior dating. (5) Furthermore, ideally the phase relationship is known between lithology and astronomical forcing parameter; as this is typically not known, all possible phase relationship should be evaluated (see section 2).

2.2 General steps of the Alpha method

The Alpha method involves two steps (Figure 1):

Step 1. Determination of the range of plausible sedimentation rate ratios (R) between the individual sedimentary facies 1 (e.g. marlstone, M in Figure 2b) and sedimentary facies 2 (e.g. limestone, L in Figure 2b). Given sedimentation rates of S_M and S_L for the two sedimentary facies, the ratio R is defined as S_M/S_L . Then R can be constrained based on assumptions 1, 2, and prior knowledge 2 (see Section 2.1).

Step 2. Prior knowledge 1 and 4 (see Section 2.1) are used in this step. Assuming that the couplets have been correctly attributed to precession (or obliquity) forcing, they should preserve the frequency modulation that is characteristic of the theoretical precession (or obliquity). We seek to evaluate the match between the predicted and observed frequency modulation, given the range of plausible R values identified in Step 1. This evaluation is conducted in the time domain with a sliding window that sequentially moves the time-calibrated record of the sequence of sedimentary couplets with facies 1 and 2 (for a given R) across the theoretical template, to test whether the expected frequency modulation is preserved. That is, a grid search is conducted across all plausible R values (from Step 1), while also evaluating all possible placements of the time-calibrated record on the target precession template. A number of metrics are used to identify the best fit R value: (Method 1) the maximum Pearson correlation between a time-calibrated record and target template and (Method 2) minimization of the standard deviation of S_M across all facies 1 layers to meet assumption 2. At the same time, the second metric will minimize the standard deviation of S_L because $S_M = S_L * R$. A combined factor (Alpha factor, Method 3), the ratio between the Pearson

correlation and standard deviation of S_M , is developed to optimize both criteria simultaneously. We name this factor the 'alpha factor'. Thus maximizing the alpha factor optimizes R and the starting precession cycle (j).

This approach builds upon principles from the Gamma method of Kominz and Bond (1990, 1992) and FM analysis (Herbert 1994; Hinnov and Park, 1998). An added merit of this approach is the evaluation of a statistical sampling of the couplets (e.g., 11 couplets, see Section 3), that allows an assessment of the consistency and variance observed in the sample set (e.g., similar number of laminae in couplets, etc.; see Section 3 and Table 3).

2.3 Model simulation

To test the performance of the Alpha method, a simulation with controlled parameters was conducted by assigning known sedimentation rates to marlstone and limestones, with cycling sedimentation according to the precession index model from the La2004 astronomical solution (Laskar et al, 2004). The Alpha method was applied to this synthetic model to determine its success in reconstructing the defined facies-specific sedimentation rates.

2.3.1 Synthetic data

The standardized precession index model ($e \cdot \sin \omega$) of the La2004 solution was extracted from 96.27-96.85 Ma of the *etp* function in the *astrochron* R package (Meyers 2014) (Figure 2a), the same interval as the Eagle Ford Formation case study (Section 3). While theoretical astronomical solutions are not valid in detail for such ancient records, general properties of the solutions are assumed to apply, specifically, the FM of the precession index by the orbital eccentricity. Errors in precession frequency k results in an uncertainty in the reconstructed sedimentation duration in

the case studies (Sections 3 and 4). For this first synthetic case study, however, we assume no uncertainty in k as defined by Laskar et al. (2004).

In the synthetic model, limestones are set to form during precession index minima (troughs), when summer insolation is high and pelagic carbonate productivity is at a maximum. The durations between troughs in the precession index are used to estimate the FM (Figure 2a). In total, 27 cycles are identified, and their durations are assembled into vector P, in kiloyears.

- P = (23, 21, 21, 20, 18, 18, 21, 24, 22, 22, 21, 21, 23, 23, 22, 21, 20, 21, 27, 22, 21, 18, 18, 18, 20,
- 166 20, 21)

The climate threshold for deposition of limestone (versus marlstone) is proscribed to be at standardized $e \cdot \sin \omega = -1$, which correlates with high insolation. Thus, for values less than standardized $e \cdot \sin \omega = -1$, limestone is deposited, whereas marlstone is deposited when it is greater than -1. Eight cycles were selected from the precession index model (Figure 2a): from i1 to i2, i3 to i4, ..., and i17 to i18 limestone is deposited, whereas from i2 to i3, i4 to i5, ..., and i16 to i17 marlstone is deposited. The thickness of each unit (from M1 to L9 in Figure 2b) is obtained from the modeled sedimentation rates of 1 cm/kyr for marlstone units and 3 cm/kyr for limestone units $(S_M=1 \text{ cm/kyr}, S_L=3 \text{ cm/kyr}).$

M1 to L9 represent the simulated result of a set of marlstone/limestone couplets. We then define the following vectors:

- 180 *marlT*= (thickness of M1, M2, M3, M4, M5, M6, M7, M8)
- lime $T = \frac{\text{(thickness of } (L1+L2)/2, }{(L2+L3)/2, }{(L3+L4)/2, }{(L3+L4)/2, }{(L4+L5)/2, }{(L5+L6)/2, }{(L6+L7)/2, }$
- 182 (L7+L8)/2, (L8+L9)/2)
- and the duration of cycles C1 to C8 as C = (22, 21, 21, 23, 23, 22, 21, 20).

185

2.3.2 Testing the synthetic model with the Alpha method

- 186 The Alpha method is applied to this synthetic model to test the validity of the technique.
- Assumptions 1, 2 and 3 are valid; prior knowledge for the synthetic data is: The couplets are
- influenced by the precession index; the sedimentation rate (SR) of each facies is bounded between
- 189 0.5 cm/kyr and 5 cm/kyr; the constraint for couplet periodicity is from 15 to 30 kyr; and the La2004
- 190 (Laskar et al., 2004) precession index is chosen for evaluation of the synthetic data.

191

192 Step 1: Constraining *R*

- Constraints for $R = S_M/S_L$ are obtained by running the R code in Section 1 of the Supplementary
- Material 1, and are shown in Figure 2c: 0.14 < R < 5.6

195

196 Step 2: Optimizing R

- The time represented by cycles from C'1 to C'8 (defined as vector C') should be correlated with
- the cycles from C1 to C8. The true time represented by C', TC'= (limeT/ S_L +marlT/ S_M), should
- have the highest alpha factor, the highest Pearson correlation, and the lowest standard deviation of
- 200 S_M .

- Following execution of the code in Section 2 of the Supplementary Material 1, the optimal fit shows that
- 203 the 10th precession index cycle has the highest correlation with the first marlstone/limestone couplets in all

three misfit criteria. The optimized **R** is 0.29, 0.28 and 0.28 for the Method 1, Method 2 and Method 3, respectively (Figure 2d). The true R is 0.33 and the starting precession cycle (j) is the 10^{th} ($S_M=1$ cm/ka, S_L =3 cm/ka; Figure 2b), which is close to the reconstructed results mentioned above. The discrepancy is caused by the fact that the trough in the true precession index cycle $(e \cdot \sin \omega)$ is not precisely at the midpoint of the simulated limestone (for example, the first trough of C1 is not at the midpoint between i1 and i2, see Figures 2a, b), which produces the time differences between C1-C8 and C'8-C'8 (Table 1). This error ranges from 0.24% to 2.57% (Table 1). Comparing the results of the reconstructed ratio *R*=0.28 (model test result) and the true R=0.33 (Table 1), the duration for the marlstone in the model is within 7% error. Together with the 1.8% error from the precession duration in the studied interval, the total error could be up to 7.2% by summing all errors in quadrature (square root of the sum of squares) for duration estimates of the geological record. The sedimentation rates for the marlstone and limestone are 0.94 to 0.97 cm/kyr and 3.34 to 3.45 cm/kyr, respectively (Table 1). To assess the power and sensitivity of the Alpha method, the wrong phase was also tested. The C1 to C8 are the cycles from the trough to trough of the precession index (Figure 2). In the wrong phase test, the Alpha method was run by using the precession index cycles determined by peak to peak (Figure 1a', R code in Section 3 of the Supplementary Material 1). The results of right phase have higher Pearson correlation and Alpha factor, and lower standard deviation (Table 2). The results from different metrics based on the right phase are more consistent than that using wrong phase. For example, the start correlating cycle number obtained based on the wrong phase test is 15 in Method 1 comparing to 10 (true value) in other two statistics (Table 2). So the wrong phase relationship from assuming peak-topeak can be rejected by using the Alpha method. This demonstrates the ability of Alpha method to determine the right phase relationship between sedimentary facies and astronomical cycles.

225

226

227

204

205

206

207

208

209

210

211

212

213

214

215

216

217

218

219

220

221

222

223

224

3. Case study 1: Middle Cenomanian Eagle Ford Formation

The Iona-1 core from west Texas, USA preserves precession-forced limestone/marlstone couplets from 141-146 m (Eldrett et al., 2015a, Figure 3). Prior investigation of this stratigraphic unit (Eldrett et al., 2015a) identified a series of 14 precession cycles through the interval (L1 to L12, Figure 3b). Robust assessment of sub-precession scale variability requires additional time constraints. We provide these time constraints by applying the Alpha method to evaluate limestone vs. marlstone sedimentation rates. We assume that the facies-specific sedimentation rates are approximately constant across all 14 couplets, which is supported by the observation that limestone-marlstone couplets represent self-similar precession cycles and have similar thickness of laminae in the marlstone units (Table 3). These mm-scale laminae are preserved in each marlstone unit (Figure 3d). As discussed further below, we will leverage the laminae, as a key constraint for application of the Alpha method.

The astronomical model is the La2004 astronomical solution (Laskar et al. (2004). The sedimentation rates of the limestone and marlstone facies are estimated to be bounded between 0.5 cm/kyr and 5 cm/kyr. The time for each marlstone/limestone couplet represents a precession cycle (Eldrett et al. 2015b), which can take on periods ranging from 15 to 30 kyr due to FM of the precession index.

Based on the 405 kyr astronomical time scale and the closest bentonite to the 141-146 m interval used as the anchor (B7, 95.80 ± 0.14 Ma) (Eldrett et al., 2015a), the age at 141 m is 96.41 ± 0.14 Ma. Applying an average sedimentation (compacted rock accumulation) rate of 1.67 cm/kyr (Eldrett et al., 2015a), the duration of the 141-146 m interval is \sim 0.3 Myr. Thus, considering the age and its uncertainty, the 141-146 m interval is between 96.27-96.85 Ma. Using the *etp* function

in the *astrochron* R package (Meyers 2014), the La2004 precession index model with a time resolution of 1 kyr is extracted for this time interval.

3.1 The Alpha method applied to the Iona-1 core

The limestone and marlstone units within the 141-146 m interval are designated as L1-L12 and M1-M11, respectively (Figure 3c). The number of laminae pairs in each marlstone is counted based on the high-resolution core photos (Figure 3d), and the average thickness for the laminae pairs of each marlstone ranges from 1.95-2.33 mm (Table 3). This observation supports a common periodic origin of the laminae pairs, and similar sedimentation rates for each marlstone. This approach assumes that the FM preserved in the theoretical precession index solution is generally valid for the Cretaceous. However, the amplitude and phase of the precession index are not constrained for the Cretaceous (Berger et al., 1992; Laskar et al., 2004), so this approach can only provide an approximate analog, and cannot be used to "anchor" the chronology.

The limestone/marlstone units spanning 141-146 m in the Iona-1 core have been demonstrated to represent precession-driven cycles, and the limestone lithofacies is interpreted to form during higher insolation/lower precession due to carbonate productivity model (Eldrett et al., 2015a, 2015b). Thus, the time of deposition between the middle of two limestones should be correlated with the time from one precession index trough to the next precession index trough (insolation peak, Hinnov and Hilgen, 2012). In a few cases, there may not be a limestone deposited at a precession index trough, due to an eccentricity amplitude modulation trough that precludes achievement of the threshold (Eldrett, et al., 2015b); this can result in a longer (thicker) deposition

of limestone and marlstone units. Such cases are found in the 141-146 m interval (M1 and M2, Figure 3).

275

276

277

278

279

280

281

282

283

284

285

286

287

288

289

290

273

274

The median number of laminae pair counts of each marlstone is 87, and the ratios between the number of laminae pairs in each marlstone with the median value are 1.8 (M1), 3.0 (M2), 0.9 (M3), 1.4 (M4), 0.4 (M5), 0.9 (M6), 1.2 (M7), 2.9 (M8), 0.8 (M9), 1.0 (M10), 1.0 (M11) (Figure 3d, Table 3). The median value is the most consistent value (6 out of 11: M3, M6, M7, M9, M10, M11) and has an integer, or close to integer, ratio with 3 of the marlstone layers (M1, M2, M8). Only two of the marlstone layers have ratios falling between integers (M4 and M5). Thus, if the median 87 laminae pair count represents the average precession-driven cycle – and if the laminae themselves are temporally self-consistent (e.g., representing some quasi-periodic time scale) – then M1 constitutes 2-precession cycles, and M2 and M8 both represent 3-precession cycles. The M5 ratio is much less than 1, which may indicate that sediment is missing from this cycle possibly due to erosion. The M4 ratio is 1.4, between 1 and 2, which is explained as representing a 2-precession cycle with some missing sediment. These two cycles (M4 and M5) were excluded from the Alpha method, due to this evidence of notable missing time. Thus, the couplets from L1 to L12 are interpreted to represent 17 precession cycles instead of the 14 originally identified by Eldrett et al. (2015a).

291

292

293

294

3.1.1. Determining the total range of plausible sedimentation rate ratios (R).

The times of L-M couplets and the precession index model are compared to determine the time distribution between the limestone and the marlstone in the 141-146 m interval (Figure 4a).

- The relevant vectors for each couplet in the 141-146 m interval, excluding M4 and M5, are:
- 297 $M_L = [(M1/S_M + (L1+L2)/2/S_L), (M2/S_M + (L2+L3)/2/S_L), (M3/S_M + (L3+L4)/2/S_L),$
- 298 $(M6/S_M+(L6+L7)/2/S_L), (M7/S_M+(L7+L8)/2/S_L), (M8/S_M+(L8+L9)/2/S_L),$
- 299 $(M9/S_M+(L9+L10)/2/S_L), (M10/S_M+(L10+L11)/2/S_L), (M11/S_M+(L11+L12)/2/S_L)]$
- 300 *marlT*=[M1, M2, M3, M6, M7, M8, M9, M10, M11] (in thickness)
- 301 $lime T = \frac{(L1+L2)}{2}, \frac{(L2+L3)}{2}, \frac{(L3+L4)}{2}, \frac{(L6+L7)}{2}, \frac{(L7+L8)}{2}, \frac{(L8+L9)}{2}, \frac{(L9+L10)}{2},$
- 302 (L10+L11)/2, (L11+L12)/2] (in thickness)
- Then $M_L = marlT / S_M + limeT / S_L$
- Since $S_L = S_M/R$, then:
- 305 $M_L = marlT / S_M + limeT / S_M * R = (marlT + limeT * R) * (1/S_M)$
- 306 Define $M_{L'} = marlT + limeT*R$
- 307 Then $M_L = (1/S_M)^* M_{L}$,

311

- $R = S_M/S_L$ is constrained to be between 0.18 and 1.37 (Figure 4b) by running the code in Section 1
- of the Supplementary Material 2.
- 3.1.2. Determining optimal R by performing a grid search across plausible values
- Here we shift the possible $R=S_M/S_L$ obtained in Step 1, and the first correlating cycle number (j)
- in the precession index model with the L-M couplets, to maximize the alpha factor and Pearson
- 315 correlation, and minimize the standard deviation of S_M .
- 317 Given the possible time duration of L-M, 27 precession index cycles (peak to peak) are defined in
- a vector P = P[n] (n=1, 2, 3, ..., 26, 27) (Figure 3a). 17 consecutive numbers are selected from P

to form a 9-number sequence (vector **P.i**): the 1st and 2nd numbers in **P.i** are summed (2-precession cycles amalgamated), the 3th to 5th number in the **P** are summed (3-precession cycles amalgamated), the 7th to 9th number in **P.i** should be skipped (for the M4 and M5 cycles, see above) and the 12th to 14th number are summed as one number (2-precession cycles amalgamated).

- $\mathbf{P.i} = [\mathbf{P}[i] + \mathbf{P}[i+1], \mathbf{P}[i+2] + \mathbf{P}[i+3] + \mathbf{P}[i+4], \mathbf{P}[i+5], \mathbf{P}[i+9], \mathbf{P}[i+10], \mathbf{P}[i+11] + \mathbf{P}[i+12] + \mathbf{P}[i+13],$
- **P**[i+14], **P**[i+15], **P**[i+16]]
- Where "i" are integers from 1 to 11.

By shifting the possible $R=S_M/S_L$ obtained in Step 1 and shifting i from 1 to 11, the optimal fit between P.i and $M_{L'}$ (the highest alpha factor, the highest positive Pearson correlation between P.i and $M_{L'}$ and smallest standard deviation of S_M) can be found to determine the value of R and J. Then the time distribution between the limestones and the marlstones in the 141-146 m interval can be solved to calculate the duration for the laminae pair in the marlstones.

The prior phase relationship we determined and the reverse phase relationship are both investigated to verify our prior (Section 2 and 3 of the Supplementary Material 2). The reverse phase relationship is that the precession index high correlates the formation of limestone. The statistics of the prior phase are higher (Table 4), which demonstrates that our prior phase relationship is valid. Using the prior phase relationship, the optimal fit in all three metrics shows a consistent starting precession cycle number, 9 (Figure 4c). The optimized R is 0.24, 0.18 and 0.18 based on the Method 1, Method 2 and Method 3, respectively (Figure 4c). The discrepancy of R using different metrics may result from the influence of non-periodic signals in the record. Such

discrepancy was also seen in the simulated test in Section 2.3. Here we select 0.18 as the best one based on the latter two metrics. By applying R=0.18, the time distribution and sedimentation rate for the marlstone/limestone couplets can be obtained (Table 3). Thus, the time represented by the laminae pairs range from 198 ± 17 year to 260 ± 23 year (Table 3), which is similar to the de Vries solar cycle (~200 year, Wagner et al., 2001). Further investigation of this possible solar cycle will be discussed in a separate paper (Ma et al., in preparation).

348

349

350

351

352

353

354

355

356

357

358

359

360

361

362

363

364

342

343

344

345

346

347

Thus, the first L-M couplet correlates with the 9th precession index cycle from top to bottom (Figure 3a). Dashed lines in Figures 3a-c correlate the limestone-marlstone couplets with the precession model cycles. From this, the time distribution for the limestone-marlstone couplets and their sedimentation rates are obtained (Table 3). Except for the excluded M4 and M5, S_M ranges from 0.85 to 1.02 cm/kyr and S_L ranges from 4.70 to 5.65 cm/kyr (Table 3, Figure 4e); the latter values are similar to the sedimentation rates of the overlying Austin Chalk and underlying Buda Formation in the Iona-1 core (Eldrett et al., 2015a), and relatively stable, supporting assumption 2 of the Alpha method. Our results are different from the one obtained by Lehrmann et al. (2019). They studied the Tinaja Section in Big Bend National Park, USA and recognized three main facies: chalk, mainly lime packstone to grainstone (limestone in Iona-1 core), and calcareous mudrock (marlstone in Iona-1 core). They applied the Gamma method (Kominz and Bond 1990, 1992; Kominz 1996) to facies thickness data spanning the Eagle Ford Formation to Austin Chalk of the Tinaja Section. The sedimentation rates of marlstone and limestone in their study are 0.21 cm/kyr and 1.2 cm/kyr, among which the sedimentation rate of limestone is much lower than the one we calculated (4.70 to 5.65 cm/kyr). If we apply their sedimentation rate, the durations of the limestone layers in the precession-driven cycle (Table 3) range from 300 kyr to 800 kyr, which is

unreasonable. This could be caused by two reasons: (1) Rocks in the Tinaja Section and Iona-1 core were deposited at different locations of the Western Interior Basin, and the thickness of the Eagle Ford Formation in these two locations are different (Lehrmann et al., 2019; Minisini et al., 2018). Thus, the sedimentation rates for the same facies in these two locations are likely different. (2) Lehrmann et al. (2019) assume that sedimentation rate does not change in the same facies (limestone or marlstone) throughout the entire Eagle Ford Formation at the Tinaja Section. This is not the case in the Iona-1 core, where average sedimentation rates vary between 1 to 2 cm/kyr (Eldrett et al., 2015a), which indicates that the facies-related sedimentation rates are not constant throughout the Eagle Ford Formation of the Iona-1 core.

4. Case study 2: Middle Eocene record at Expedition 342 IODP Site U1408

The Eocene deposits at IODP Site U1408 preserve dominantly obliquity-forced couplets, which consist of white nannofossil ooze (ooze layers) and greenish nannofossil-rich clay (clay layers) (Figure 5) (Boulila et al., 2018). To apply the Alpha method in this section, we picked the interval from 43-49 m, which is characterized by a relatively stable sedimentation rate (~2 cm/kyr, Boulila et al., 2018). It encompasses 7 ooze layers and 6 clay layers (O1 to O7 and C1 to C6; Figure 5d), which represent 6 obliquity cycles. The plausible range of sedimentation rates for the ooze and clay layers was set at 0.5 to 5 cm/kyr.

The sedimentation rates of ooze and clay layers are S_O and S_C , respectively, thus the ratio is $R=S_C/S_O$. The proxy that is evaluated, which records an obliquity signal in this core, is $\log(\text{Ca/Fe})$ (Figure 5e) (Boulila et al., 2018).

The challenge in this case study is that the transition between ooze and clay layers is gradual, which means that the boundaries between layers are difficult to pinpoint. Thus, a method was implemented to determine the boundaries: An assumption was made that the boundaries of the couplets are indicated by a log(Ca/Fe) threshold value. Ooze layers are above this threshold while the clay layers are below it. Possible ranges of the boundaries are indicated as the shaded bars on the log(Ca/Fe) record (Figure 5e) and core photo (Figure 5c). The threshold (label as m) was then constrained from 0.64 - 0.76 of log(Ca/Fe) (dashed lines in Figure 5e). To eliminate noise and high frequencies in log(Ca/Fe) that interfere with locating the facies boundaries (e.g., the data just below 43.5 m), lowpass filtering was applied to exclude frequencies higher than 6 cycles/m; this bandpassed curve is shown in red (Figure 5e) and was used for locating the boundaries. Changing the threshold (0.64 to 0.76 with step of 0.005) on the lowpassed data produced sets of possible thicknesses for the ooze and clay layers. The Alpha method was then applied to these sets of possible thicknesses.

The age for the study interval is from 39.062 - 39.333 Ma (Boulila et al., 2018), and is based on the \sim 0.2 Ma obliquity modulation (s_3 - s_6) period. Half of this period was used as an age uncertainty for the study interval. Hence the obliquity signal from 38.962 - 39.433 Ma is extracted from the La2004 solution (Figure 5b). The phase relationship between the obliquity and couplets are not known, thus both phase relationships are evaluated (code in the Supplementary Material 3, Table 5). The best statistics indicate that the ooze layers are formed while the obliquity is low (Table 5). The first ooze-clay couplet (mid of C1 to mid of C2) correlates with the 4^{th} obliquity peak cycle (Table 5, Figure 5). The $\log(Ca/Fe)$ threshold is 0.64 (Table 5). The sedimentation rate ratio (R) are 0.51, 0.68 and 0.67 based on Method 1, Method 2 and Method 3, respectively (Table 5). The

sedimentation rate ranges for the ooze layers are 1.56-1.69 cm/kyr and for the clay layers are 3.05-3.30 cm/kyr for Method 1; 1.71-1.85 cm/kyr (ooze) and 2.52-2.72 cm/kyr (clay) for Method 2; 1.70-1.84 cm/kyr (ooze) and 2.54-2.75 cm/kyr (clay) for Method 3 (Table 6). We recommend using the results of Method 3 because it takes both Method 1 and Method 2 into account.

5. Conclusions

The Alpha method is a robust tool for statistically evaluating the time distribution within astronomically forced limestone/marlstone couplet sequences. The method is limited to precession index or obliquity-driven couplets with facies-specific sedimentation rates. The method builds time scales by tuning stratigraphic series with astronomical solutions, correlating the midpoint of a certain lithology (e.g., limestone) with the peak or trough of precession index forcing or an obliquity model, and leveraging the frequency modulation characteristic to estimate sedimentation rates for the limestone and marlstone couplet members.

- Three assumptions are made:
- 1. No significant hiatuses are present.
- 427 2. Sedimentation rates for the limestones and marlstones are constant.
- 3. The frequency modulations of the astronomical solution plays a decisive role.
- Prior knowledge about the limestone/marlstone couplets is required:
 - 1. Couplets are influenced by precession or obliquity forcing.
 - 2. A range of plausible sedimentation rates has been determined.
- 3. Time constraints for each couplet (based on precession or obliquity forcing) is known.
 - 4. Independent age constraints for the study interval are available.

5. Phase relationship between lithology and precession or obliquity (If this is not known 434 all possible phase relationship should be assessed). 435 436 The Alpha method was applied to a synthetic stratigraphic signal and two case studies: 437 438 439 1. A synthetic precession index-forced model. This synthetic stratigraphic series forced by the precession index has marls with a sedimentation rate of 1 cm/kyr and limestones with a 440 sedimentation rate of 3 cm/kyr. The alpha method can solve the model with $\sim 7\%$ error. 441 442 2. Precession index-forced couplets of the Cretaceous Eagle Ford Formation (Iona-1 core, Texas). 443 The estimated sedimentation rates for the marlstone are 0.85-1.02 cm/kyr and for the limestone 444 are 4.70-5.65 cm/kyr (Table 3). 445 446 3. Obliquity-forced couplets of the Middle Eocene of Expedition 432, IODP Site U1408. 447 The estimated sedimentation rates for the ooze layers are 1.70-1.84 cm/kyr and for the clay layers 448 are 2.54-2.75 cm/kyr. 449 450 Sedimentary couplets may have hiatuses and/or include multiple precession index or obliquity 451 452 cycles fused together; the Alpha method provides a means to account for these complications. 453 Estimating the time scales that are internal to astronomically forced limestone and marlstone 454 455 couplet members can help constrain rates of sedimentary processes and geochemical evolution at 456 sub-Milankovitch time scales, which can be especially revelatory for key geological events such

as carbon isotope excursions. Importantly, the Alpha method can enable the exploration of climate 457 variability, paleoceanography and biotic change at time scales that are shorter than 20 kyr. 458 459 Acknowledgement 460 This study was supported by the National Natural Science Foundation of China (Grant No. 461 41888101), U.S. NSF Grant EAR-1151438 (S.R.M.) and OAC-1835717. We thank David 462 DeVleeschouwer for valuable comments that improved this work. 463 Reference 464 Abels H. A., Abdul Aziz H., Ventra D., Hilgen F. J., 2009a. Orbital climate forcing in mudflat to 465 marginal lacustrine deposits in the Miocene Teruel Basin (North-East Spain). Journal of 466 Sedimentary Research 79:831–847. 467 Abels H. A., Abdul Aziz H., Calvo J. P., Tuenter E., 2009b. Shallow lacustrine carbonate 468 microfacies document orbitally paced lake-level history in the Miocene Teruel basin 469 (North-East Spain). Sedimentology 56:399–419. 470 471 Adams, T.D., Khalili, M. and Said, A.K. 1967. Stratigraphic significance of some oligosteginid assemblages from Lurestan Province, northwest Iran. Micropaleontology, 13, 55-67. 472 Batenburg, S.J., De Vleeschouwer, D., Sprovieri, M., Hilgen, F.J., Gale, A.S., Singer, B.S., 473 Koeberl, C., Coccioni, R., Claeys, P. and Montanari, A., 2016. Orbital control on the timing 474 of oceanic anoxia in the Late Cretaceous. Climate of the Past, 12(10), pp.1995-2009. 475 Berger, A., Loutre, M.F. and Laskar, J., 1992. Stability of the astronomical frequencies over the 476 Earth's history for paleoclimate studies. Science, 255(5044), pp.560-566. 477

Boulila, S., Vahlenkamp, M., De Vleeschouwer, D., Laskar, J., Yamamoto, Y., Pälike, H., Turner,

S.K., Sexton, P.F., Westerhold, T. and Röhl, U., 2018. Towards a robust and consistent

478

- middle Eocene astronomical timescale. Earth and Planetary Science Letters, 486, pp.94-
- 481 107.
- Davies, A., Kemp, A.E.S., and Pike, J., 2009, Late Cretaceous seasonal ocean variability from the
- 483 Arctic: Nature, v. 460, p. 254–258.
- Dias-Brito, D., 2000. Global stratigraphy, palaeobiogeography and palaeoecology of Albian-
- 485 Maastrichtian pithonellid calcispheres: impact on Tethys configuration. Cretaceous
- 486 Research, 21: 315-349.
- Dinarès-Turell, J., Baceta, J.I., Pujalte, V., Orue-Etxebarria, X., Bernaola, G. and Lorito, S., 2003.
- 488 Untangling the Palaeocene climatic rhythm: an astronomically calibrated Early Palaeocene
- magnetostratigraphy and biostratigraphy at Zumaia (Basque basin, northern Spain). Earth
- and Planetary Science Letters, 216(4), pp.483-500.
- Donovan, A.D., Staerker, T.S., Pramudito, A., Li, W., Corbett, M.J., Lowery, C.M., Romero, A.M.
- and Gardner, R.D., 2012. The Eagle Ford outcrops of West Texas: a laboratory for
- 493 understanding heterogeneities within unconventional mudstone reservoirs.
- Eldrett, J.S., Ma C., Bergman, S.C. Lutz B., Gregory, J., Dodsworth, P., Phipps M., Hardas P.,
- 495 Minisini, D., Ozkan, A., Ramezani, J., Bowring, S.A., Kamo, S.L., Ferguson, K.,
- Macaulay, C., Kelly, A.E., 2015a, An astronomically calibrated stratigraphy of the
- 497 Cenomanian, Turonian and earliest Coniacian from the Cretaceous Western Interior
- 498 Seaway, USA: Implications for global chronostratigraphy: Cretaceous Research, v. 56,
- p.316-344.
- 500 Eldrett, J.S., Ma, C., Bergman, S.C., Ozkan, A., Minisini, D., Lutz, B., Jackett, S.-J., Macaulay,
- 501 C., Kelly, A.E., 2015b. Origin of limestone–marlstone cycles: astronomic forcing of

502 organic-rich sedimentary rocks from the Cenomanian to early Coniacian of the Cretaceous Western Interior Seaway, USA. Earth Planet. Sci. Lett. 423, 98–113. 503 Fischer, A.G., 1986. Climatic rhythms recorded in strata. Annual Review of Earth and Planetary 504 Sciences, 14(1), pp.351-376. 505 Hilgen, F.J., Krijgsman, W., Langereis, C.G., Lourens, L.J., Santarelli, A. and Zachariasse, W.J., 506 507 1995. Extending the astronomical (polarity) time scale into the Miocene. Earth and Planetary Science Letters, 136(3-4), pp.495-510. 508 Hilgen, F.J., Hinnov, L.A., Aziz, H.A., Abels, H.A., Batenburg, S., Bosmans, J.H., de Boer, B., 509 510 Hüsing, S.K., Kuiper, K.F., Lourens, L.J. and Rivera, T., 2014. Stratigraphic continuity and fragmentary sedimentation: the success of cyclostratigraphy as part of integrated 511 stratigraphy. Geological Society, London, Special Publications, 404, pp.SP404-12. 512 513 Herbert, T.D., 1994. Reading orbital signals distorted by sedimentation: models and examples. Orbital forcing and cyclic sequences, pp.483-507. 514 Hinnov, L.A. and Park, J., 1998. Detection of astronomical cycles in the stratigraphic record by 515 frequency modulation (FM) analysis. Journal of Sedimentary Research, 68(4), pp.524-539. 516 Hinnov, L.A., and Hilgen, F.J., 2012, Chapter 4: Cyclostratigraphy and astrochronology, in 517 518 Gradstein, F., Ogg, J., Ogg, G., and Smith, D., eds., A Geologic Time Scale 2012: Amsterdam, Elsevier, p. 63–83. 519 Hinnov, L.A., 2013. Cyclostratigraphy and its revolutionizing applications in the earth and 520 521 planetary sciences. GSA Bulletin, 125(11-12), pp.1703-1734. Hinnov, L.A., 2018. Chapter 1: Cyclostratigraphy and Astrochronology in 2018. Stratigraphy and 522

523

Timescales, v. 3, p. 1-80.

Kominz, M.A. and Bond, G.C., 1990. A new method of testing periodicity in cyclic sediments: 524 application to the Newark Supergroup. Earth and Planetary Science Letters, 98(2), pp.233-525 244. 526 Kominz, M.A. and Bond, G.C., 1992. Documenting the reliability and utility of the γ method as 527 applied to cyclic sections using forward modeling. Earth and Planetary Science Letters, 528 529 113(3), pp.449-457. Kominz, M.A., 1996. Whither cyclostratigraphy? Testing the Gamma Method on Upper 530 Pleistocene deep-sea sediments, North Atlantic Deep Sea Drilling Project Site 609. 531 Paleoceanography, 11(4), pp.481-504. 532 Krijgsman W., Hilgen F. J., Langereis C. G., Santarelli A., Zachariasse W. J., 1995. Late Miocene 533 magnetostratigraphy, biostratigraphy and cyclostratigraphy from the Mediterranean. Earth 534 and Planetary Science Letters 136:475–494. 535 Kuiper, K.F., Deino, A., Hilgen, F.J., Krijgsman, W., Renne, P.R. and Wijbrans, A.J., 2008. 536 Synchronizing rock clocks of Earth history. science, 320(5875), pp.500-504. 537 Laskar, J., Robutel, P., Joutel, J., Gastineau, M., Correia, A.C.M., and Levrard, B., 2004, A 538 numerical solution for the insolation quantities of the Earth: Astronomy & Astrophysics, 539 540 v. 428, p. 261–285, doi:10.1051/0004-6361:20041335. Lehrmann, D.J., Yang, W., Sickmann, Z.T., Ferrill, D.A., McGinnis, R.N., Morris, A.P., Smart, 541 542 K.J. and Gulliver, K.D., 2019. Controls On Sedimentation and Cyclicity of the Boquillas 543 and Equivalent Eagle Ford Formation from Detailed Outcrop Studies of Western and Central Texas, USA. Journal of Sedimentary Research, 89(7), pp.629-653. 544

Ma, C., Meyers, S.R., Sageman, B.B., Singer, B.S. and Jicha, B.R., 2014. Testing the astronomical 545 time scale for oceanic anoxic event 2, and its extension into Cenomanian strata of the 546 Western Interior Basin (USA). Bulletin, 126(7-8), pp.974-989. 547 Ma, C., Eldrett J.S., Meyers, S.R., Bergman, S.C., Minisini, D., Lutz, B., Hinnov, L.A., 2020. 548 Centennial scale solar forcing of hothouse climates during the Mid-Cenomanian Event, in 549 550 preparation. Meyers, S.R. (2014). Astrochron: An R Package for Astrochronology. https://cran.r-551 project.org/package=astrochron. 552 553 Minisini, D., Eldrett, J., Bergman, S.C. and Forkner, R., 2018. Chronostratigraphic framework and depositional environments in the organic-rich, mudstone-dominated Eagle Ford Group, 554 Texas, USA. Sedimentology, 65(5), pp.1520-1557. 555 556 Paillard, D., Labeyrie, L. and Yiou, P., 1996, Macintosh program performs time-series analysis, EOS Transactions AGU, Vol. 77, p. 379. 557 Research On Cretaceous Cycles Group (ROCC), 1986, Rhythmic bedding in Upper Cretaceous 558 pelagic carbonate sequences: Varying sedimentary response to climatic forcing. Geology, 559 Vol. 14, pp. 153-156. 560 561 Wagner, G., Beer, J., Masarik, J., Muscheler, R., Kubik, P.W., Mende, W., Laj, C., Raisbeck, G.M. and Yiou, F., 2001. Presence of the solar de Vries cycle (~ 205 years) during the last ice 562 age. Geophysical Research Letters, 28(2), pp.303-306. 563 Westphal, H., Hilgen, F. and Munnecke, A., 2010. An assessment of the suitability of individual 564 rhythmic carbonate successions for astrochronological application. Earth-Science 565 Reviews, 99(1-2), pp.19-30. 566

567	Westphal, H., Munnecke, A., Böhm, F. and Bornholdt, S., 2008. Limestone-marl alternations in
568	epeiric sea settings - witnesses of environmental changes of diagenesis, Geological
569	Association of Canada Special Paper 48, 1-18.
570	Westphal, H. and Munnecke, A., 2003. Limestone-marl alternations: A warm-water phenomenon?
571	Geology, 31: 263-266.
572	Zeeden C., Hilgen F., Westerhold T., Lourens L., Röhl U., Bickert T. (2012) Revised Miocene
573	splice, astronomical tuning and calcareous plankton biochronology of ODP Site 926
574	between 5 and 14.4 Ma. Palaeogeography, Palaeoclimatology, Palaeoecology 369:430-
575	451.

Table 1. Model test result, where $S_M = 1$ cm/kyr and $S_L = 3$ cm/kyr in the synthetic model. Please note that marlT + limeT is C'1-C'8 (lithology couplets, Figure 1b), whose correlated time has small difference from C1-C8 (precession index cycles, see section 2.3).

	Model	: $S_M = 1 \text{ cm/ky}$	V_{r} , S_{L} =3 cm/k	$yr, \mathbf{R} = 0.3$	33		Results from the Alpha method: $R = 0.28$ Precession index cycles are trough-to-trough (right phase)				
Marlstone/ limestone couplets	Precession index cycles (kyr)	Actual duration of marlT (kyr)	Actual duration of limeT (kyr)	marlT (cm)	limeT (cm)	Duration of marlT (kyr)	Error for duration of marlT	Duration of limeT (kyr)	Error for duration of limeT	S _M (cm/kyr)	S _L (cm/kyr)
C'1	C1 = 22	16.52	5.26	16.52	15.79	17.35	5.02%	4.65	-11.60%	0.95	3.40
C'2	C2 = 21	13.83	7.04	13.83	21.13	14.71	6.36%	6.29	-10.65%	0.94	3.36
C'3	C3 = 21	13.61	7.28	13.61	21.84	14.49	6.47%	6.51	-10.58%	0.94	3.35
C'4	C4 = 23	15.95	6.62	15.95	19.86	17.05	6.90%	5.95	-10.12%	0.94	3.34
C'5	C5 = 23	16.76	6.36	16.76	19.08	17.44	4.06%	5.56	-12.58%	0.96	3.43
C'6	C6 = 22	15.33	6.92	15.33	20.75	15.95	4.04%	6.05	-12.57%	0.96	3.43
C'7	C7 = 21	13.58	7.47	13.58	22.41	14.36	5.74%	6.64	-11.11%	0.95	3.38
C'8	C8 = 20	13.22	7.29	13.22	21.88	13.67	3.40%	6.33	-13.17%	0.97	3.45

Table 2. Best statistics and results from Alpha method applied to synthetic model. The modeled R (sedimentation rates' ratio) is 0.33 and j (the start correlating cycle number) is 10.

Phase relationship		Pearson correlation	Standard deviation	Alpha factor
Precession low -	Best statistics	0.9677076	0.01188799	81.39882
limestone (right phase)	Results based on best statistics	R = 0.29, j = 10	R = 0.28, j = 10	R = 0.28, j = 10
Precession high -	Best statistics	0.9051734	0.02644401	32.59319
limestone (wrong phase)	Results based on best statistics	R = 0.26, j = 15	R = 0.34, j = 10	R = 0.35, j = 10

Table 3. The result of limestone and marlstone couplets from 141-146 m in the Iona-1 core. B is the thickness of A (limestone bed). D is the thickness of C (Marlstone bed). E is the number of laminae pairs in C. F is the average thickness of laminae pairs in C. G is the time for A+C. H = D/L. I = H/E. J = I*7.2%. K = E/median(E). L = (D+B*R)/H/10, where R = S_M/S_L = 0.18 which is obtained by the Alpha method. M = S_M/R .

A	В	С	D	Е	F	G	Н	I	J	K	L	M
Lime- stone	Thickness of A (mm)	Marl- stone	Thicknes s of C (mm)	Numbe r of lamina e pairs in C	Average thickness of laminae pairs (mm)	Time for A+C (kyr)	Time for the marlston e (kyr)	Time for each lamina e pair (year)	Error ±7.2 %	Ratio between E and the median of all E	Marlsto ne S _M (cm/kyr)	Limeston e S _L (cm/kyr)
(L1+L2)/2	155.59	M1	344.41	160	2.15	44	40.691	255	18	1.8	0.85	4.70
(L2+L3)/2	95.34	M2	561.63	260	2.16	65	63.073	243	17	3.0	0.89	4.95
(L3+L4)/2	71.10	M3	183.52	81	2.27	23	21.501	266	19	0.9	0.85	4.74
(L4+L5)/2	85.99	M4	258.08	121	2.14	43	40.567	336	24	1.4	0.64	3.53
(L5+L6)/2	79.64	M5	82.64	35	2.34	20	17.044	482	35	0.4	0.48	2.69
(L6+L7)/2	124.77	M6	175.21	80	2.19	21	18.614	233	17	0.9	0.94	5.23
(L7+L8)/2	157.20	M7	233.84	105	2.24	27	24.085	230	17	1.2	0.97	5.39
(L8+L9)/2	107.69	M8	537.86	257	2.10	61	58.878	229	16	2.9	0.91	5.08
(L9+L10)/2	68.79	M9	151.66	68	2.22	18	16.641	243	17	0.8	0.91	5.06
(L10+L11)/2	68.56	M10	165.51	85	1.96	18	16.751	198	14	1.0	0.99	5.49
(L11+L12)/2	60.25	M11	192.52	90	2.14	20	18.933	210	15	1.0	1.02	5.65

Table 4. Best statistics and results from Alpha method applied to the Iona-1 core by using bothphase relationships.

Phase relationship		Pearson correlation	Standard deviation	Alpha factor
Precession low –	Best statistics	0.9964235	0.05866757	16.98252
limestone (better)	Results based on best statistics	R = 0.24, j = 9	R = 0.18, j = 9	R = 0.18, j = 9
D	Best statistics	0.9926746	0.06470213	15.33993
Precession high – limestone	Results based on best statistics	R = 0.26, j = 9	R = 0.18, j = 9	R = 0.18, j = 9

Table 5. Best statistics and results from Alpha method applied to the U1408 by using both phase relationships.

Phase relationship		Pearson correlation	Standard deviation	Alpha factor
Ooze layers –	Best statistics	0.9604325	0.0004892214	1945.75
obliquity low (better)	Results based on best statistics	R = 0.51, j = 4	R = 0.68, j = 4	R = 0.67, j = 4
Oogo lavana	Best statistics	0.7257793	0.0009625492	748.7346
Ooze layers – obliquity high	Results based on best statistics	R = 1.29, j = 3	R = 1.08, j = 3	R = 1.16, j = 3

Table 6. The result of ooze and clay couplets from 43-49 m in the core of Site U1408.

٨	D	D	В	D	D	D	D	D	D	D	D	D	D	D	C		Meth	nod 1			Metho	od 2			Meth	od 3	
A	В	С	D	Е	F	G	Н	I	J	K	L	M	N	О													
Ooze layer	Clay layer	Time for A+B (kyr)	Time for the A (kyr)	Time for the B (kyr)	So (cm/k yr)	S _c (cm/k yr)	Time for the A (kyr)	Time for the B (kyr)	So (cm/kyr)	S _c (cm/kyr)	Time for the A (kyr)	Time for the B (kyr)	So (cm/kyr)	S _c (cm/kyr)													
(O1+O2)/2	C1	42	11.54	30.46	3.30	1.68	14.10	27.90	2.70	1.84	13.96	28.04	2.73	1.83													
(O2+O3)/2	C2	40	11.70	28.30	3.30	1.68	14.21	25.79	2.72	1.85	14.08	25.92	2.75	1.84													
(O3+O4)/2	СЗ	36	11.82	24.18	3.17	1.62	14.21	21.79	2.64	1.79	14.08	21.92	2.66	1.78													
(O4+O5)/2	C4	39	8.86	30.14	3.31	1.69	10.99	28.01	2.67	1.81	10.87	28.13	2.70	1.81													
(O5+O6)/2	C5	42	8.84	33.16	3.30	1.69	11.02	30.98	2.65	1.80	10.90	31.10	2.68	1.80													
(O6+O7)/2	C6	38	11.25	26.75	3.05	1.56	13.65	24.35	2.52	1.71	13.52	24.48	2.54	1.70													



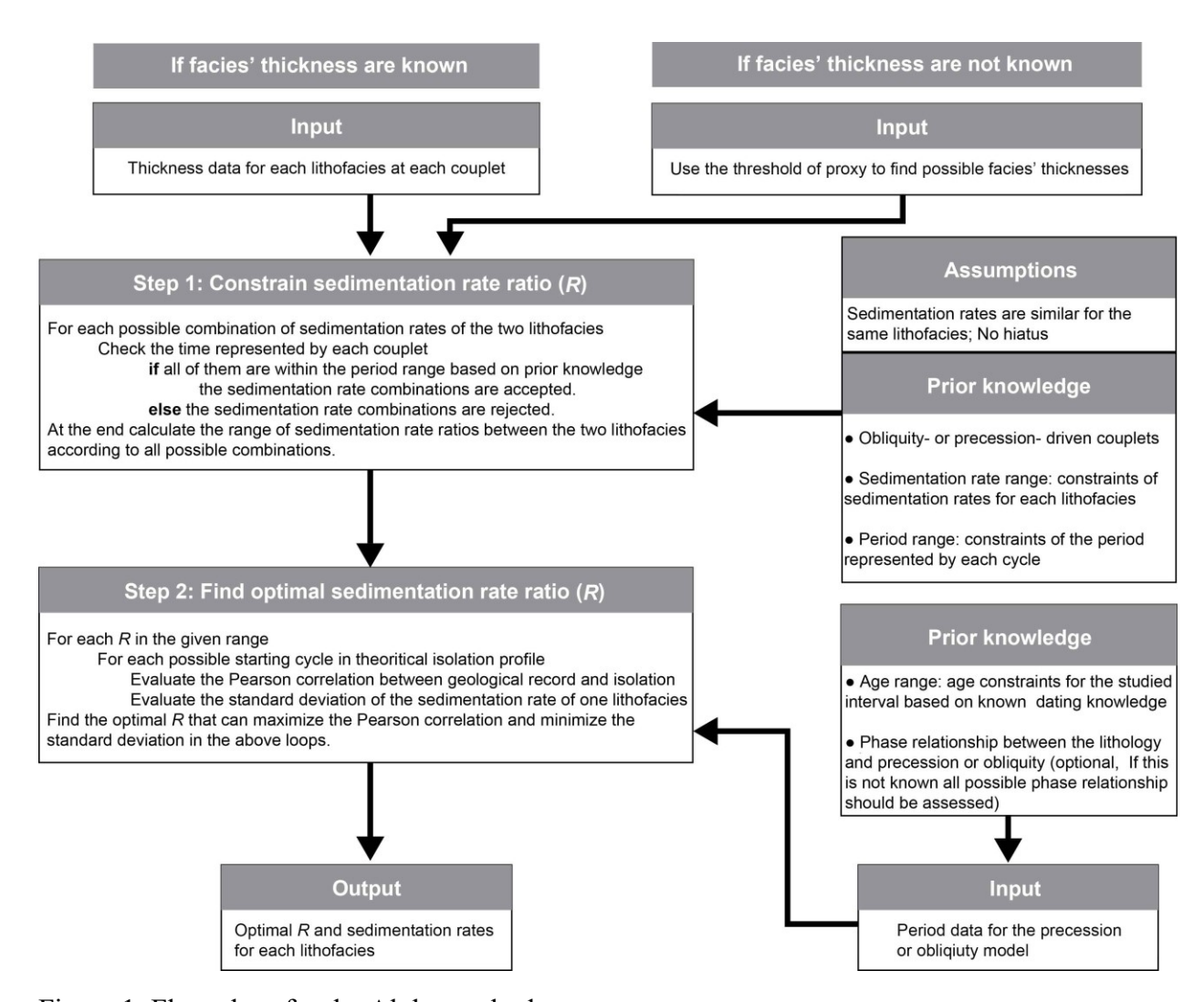


Figure 1. Flow chart for the Alpha method.

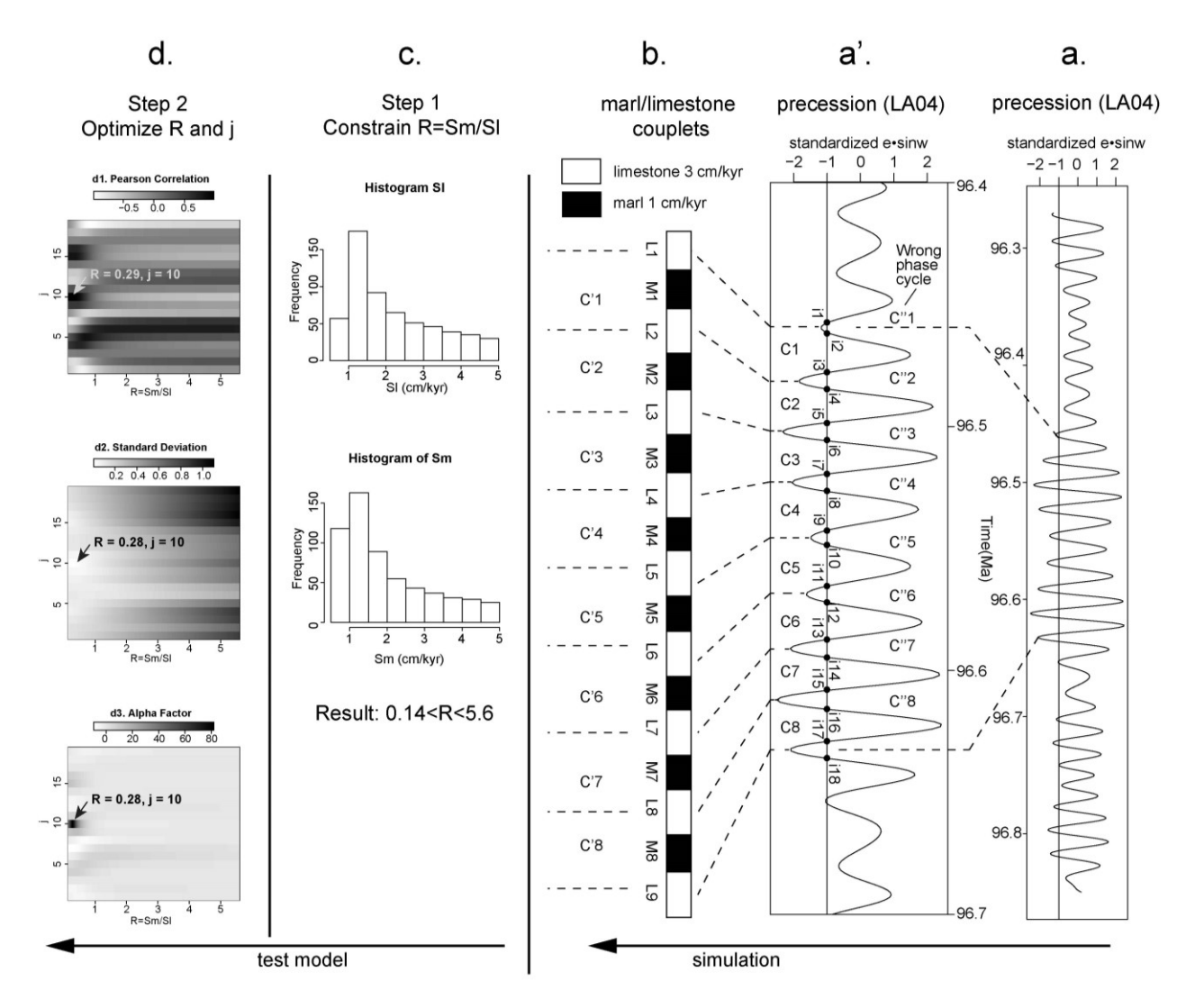


Figure 2. A model simulation and test of the Alpha method. (a) precession index model (standardized $e \cdot \sin \omega$) from 96.27-96.85Ma in the La2004 solution (Laskar et al., 2004). (a') Closer image of Figure a. Use standardized $e \cdot \sin \omega = -1$ as the threshold that forms the limestone when precession is below this value. The points of standardized $e \cdot \sin \omega = -1$ are the time when the lithology changes between the limestone and marlstone. (b) Simulated lithology formed based on (a') giving the sedimentation rate of limestone and marlstone as 3cm/kyr and 1cm/kyr respectively, 8 couplets are generated (C'1-C'8). (c) Test the model using step 1 of the Alpha method: histogram of possible S_M and S_L . The ratio of $R = S_M / S_L$ can then be constrained from 0.14-5.6. (d) Test the

model by utilizing Step 2 of the Alpha method. The X-axis stands for $R = S_M / S_L$ and the Y-axis is the jth cycle in the precession model (Figure a) correlated with the first couplet of the marlstone/limestone couplets (Figure b). Optimized R and j (automatically identified by the R code) are labeled in each image representing the three metrics defined in Section 2.2.



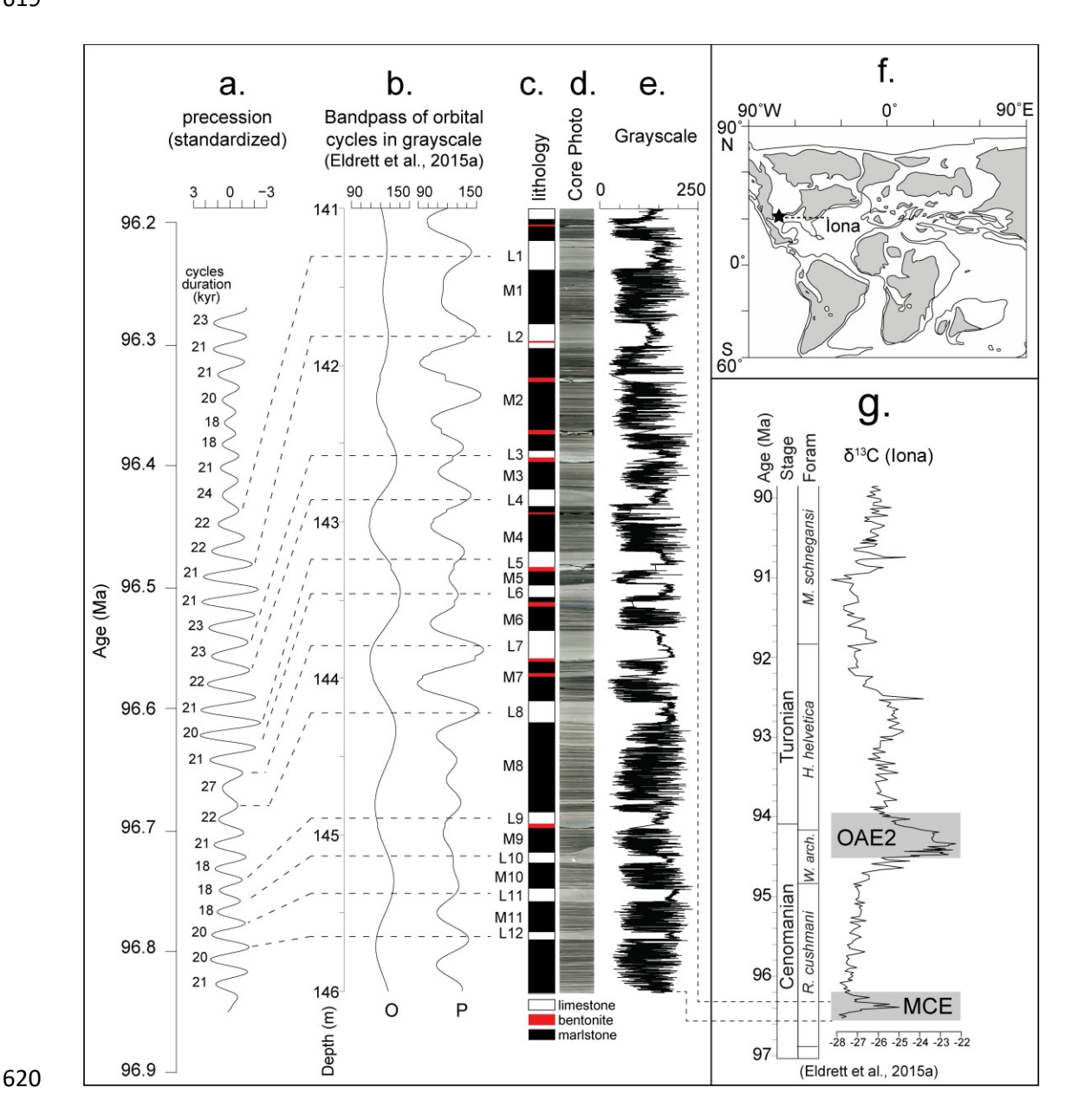


Figure 3. The Eagle Ford Formation case study. (a) Precession model for 96.27 - 96.85 Ma, from *astrochron* (Meyers, 2014), using the La2004 astronomical solution (Laskar et al., 2004). (b)

Rectangular bandpass filters of astronomical cycles in the grayscale data from 141-146 m of the Iona-1 core (O: Obliquity, P: Precession). (c) Code for each sedimentological unit. (d) Simplified lithology. (e) Grayscale data derived from core photos. (f) Cenomanian paleogeographic map (90 Ma, modified from Ron Blakey and Colorado Plateau Geosystems Inc., showing the location of the Iona-1 core (g) Carbon isotope data of the Iona-1 core organic matter fraction. The grey bars show the positions of the Mid Cenomanian Event (MCE) and OAE2 intervals in the core and the dashed lines show the 141-146 m interval. Figure (b)-(e) share the same depth scale in (b). The dashed lines that connect (a) to (c) identify precession peaks corresponding to the middle of limestone units. These dashed lines do not exactly match the precession bandpass filtered series in (b), because the bandpass filter is applied assuming a stable (constant) sedimentation rate across the limestone and marlstone (Eldrett et al., 2015a).

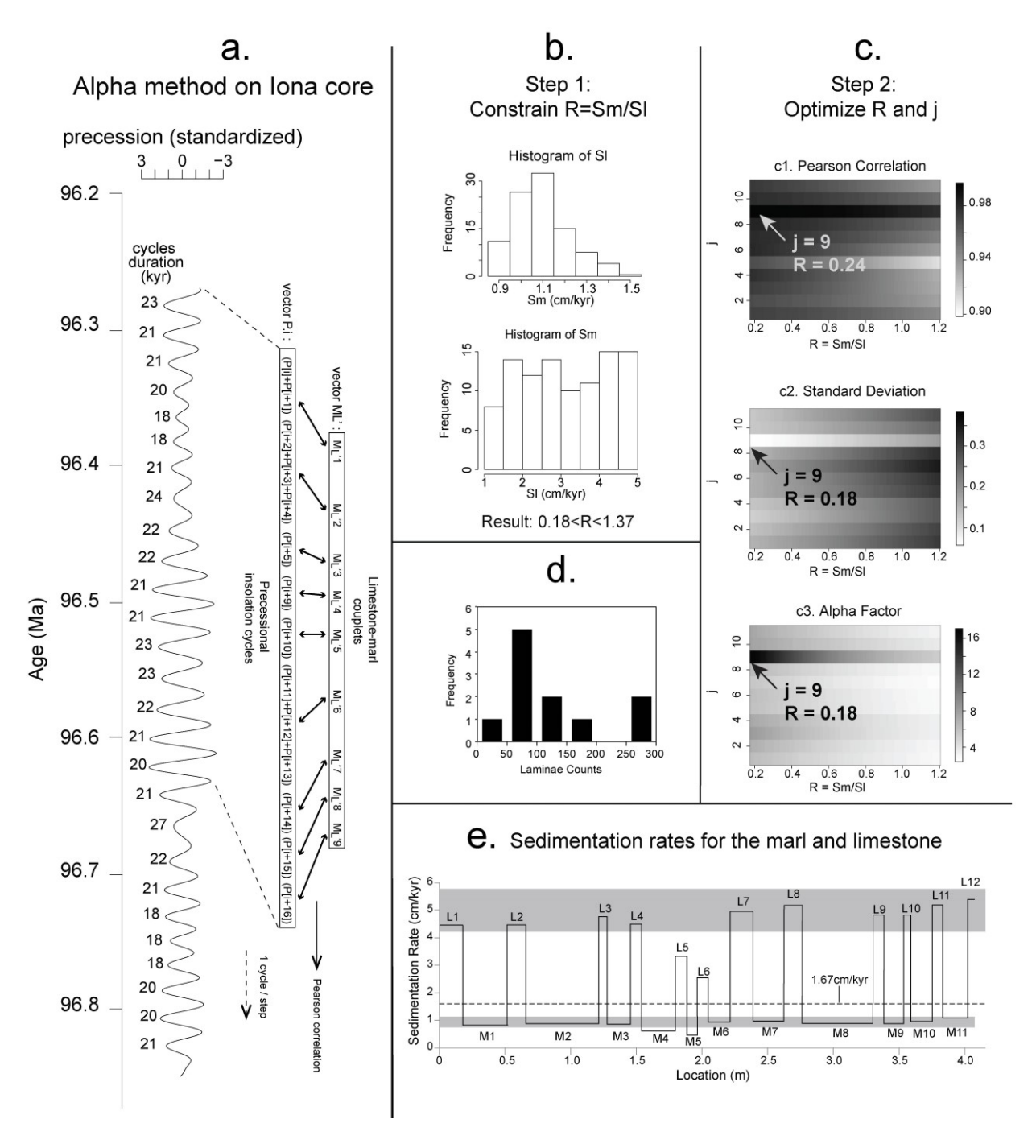


Figure 4. Alpha method applied to the Iona-1 core. (a) Illustration of the methodology. Left curve is the precession model for mid-Cenomanian based on La2004. The couplet thicknesses are matched to the sequence in the precession cycles (detail can be seen in Section 2.2). (b) Step 1: Possible combinations of S_M and S_L , considering the duration of each marlstone/limestone couplet, are constrained by the precession periods. Histogram of possible S_M and S_L is plotted and the ratio

of $R = S_M/S_L$ can be constrained as 0.18-1.37. (c) Step 2: The X-axis in the three images stands for $R = S_M/S_L$ and the Y-axis is the jth cycle of the precession cycles (Figure a). Optimized R and j are labeled in each image representing the three metrics defined in Section 2.2. (d) Histogram showing numbers of laminae pairs in all marlstone layers (M1-M11) (laminae counts: the numbers of laminae pairs, frequency: the number of marlstone layers). (e) The sedimentation rate for the marlstone and limestone layers (Table 3), the dotted line is the sedimentation rate from Eldrett et al. (2015a). The X-axis is the location relative to the top of L1 by excluding the bentonite layers.

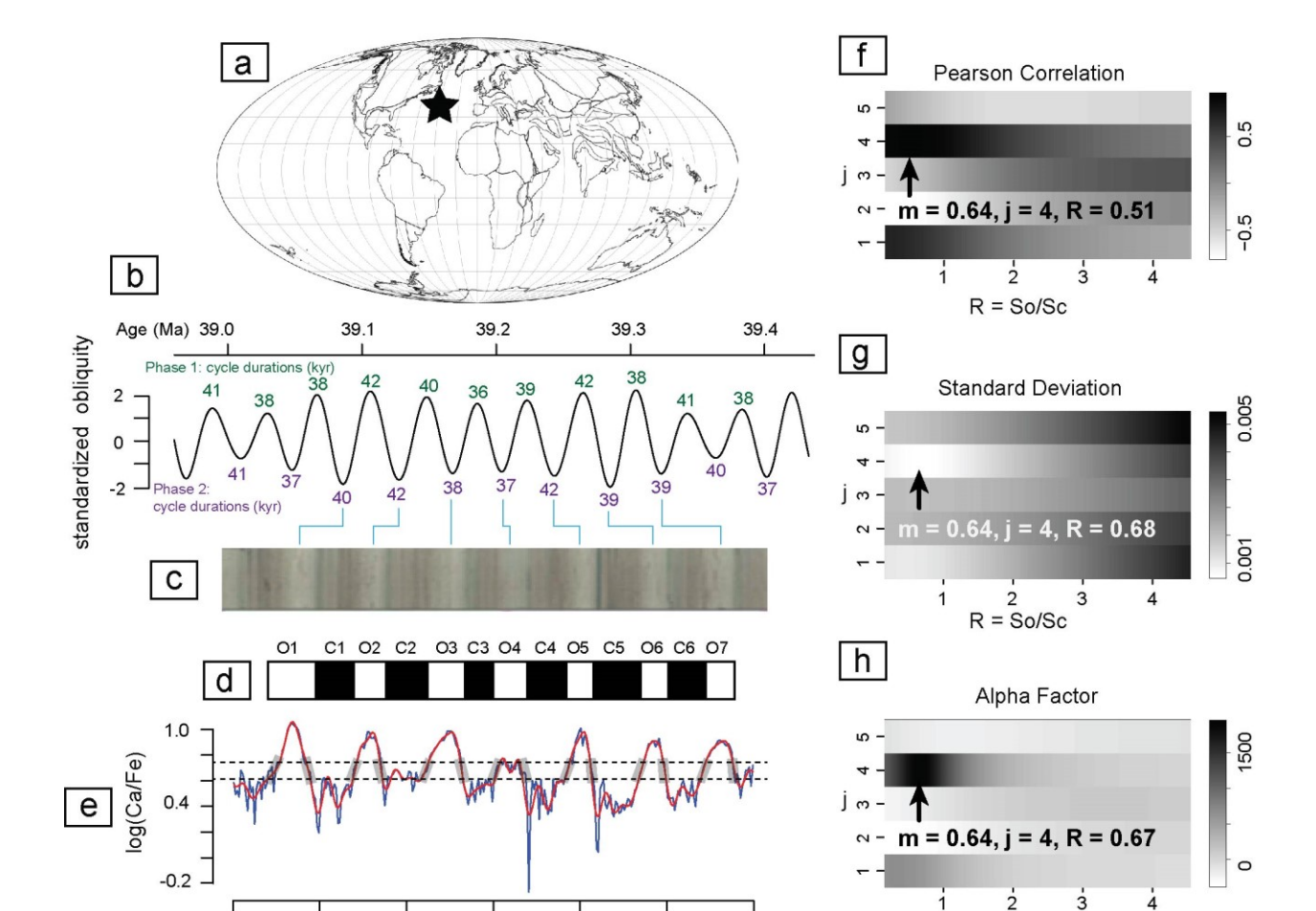


Figure 5. Alpha method applied to Site 1408. (a) Eocene paleogeographic map (40 Ma, modified from Gplate portal (http://portal.gplates.org/map/). (b) Standardized obliquity signal from 38.962

R = So/Sc

depth (m) 43

- 39.433 Ma (La2004, Laskar et al., 2004). Obliquity cycles are shown in both phase relationship:

1. obliquity low – ooze layers (green numbers) and 2. obliquity high – ooze layers (purple numbers). (c) Core photo of from 43 to 49 m of the Site 1408. (d) Simplified lithology layers and the code associated with them. Blue lines between (b) and (c) illustrate the best correlation between couplets and obliquity model. (e) Log(Ca/Fe) from 43 to 49 m of the Site 1408 (blue curve). The red curve is the lowpass filtering from blue curve. (f) Result of Method 1(g) Result of Method 2 (h) Result of Method 3. Arrows in (g)-(h) indicates the optimized result.